

## Article

# The Relationship between Soil Electrical Parameters and Compaction of Sandy Clay Loam Soil

Katarzyna Pentoś <sup>1,\*</sup> , Krzysztof Pieczarka <sup>1</sup>  and Kamil Serwata <sup>2</sup>

<sup>1</sup> Institute of Agricultural Engineering, Wrocław University of Environmental and Life Sciences, 37b Chelmońskiego Street, 51-630 Wrocław, Poland; krzysztof.pieczarka@upwr.edu.pl

<sup>2</sup> Agri Solutions Sp. z o.o., Ligota Wielka 34, 56-400 Oleśnica, Poland; k.serwata@agrisolutions.eu

\* Correspondence: katarzyna.pentos@upwr.edu.pl; Tel.: +48-71-320-5970

**Abstract:** Soil spatial variability mapping allows the delimitation of the number of soil samples investigated to describe agricultural areas; it is crucial in precision agriculture. Electrical soil parameters are promising factors for the delimitation of management zones. One of the soil parameters that affects yield is soil compaction. The objective of this work was to indicate electrical parameters useful for the delimitation of management zones connected with soil compaction. For this purpose, the measurement of apparent soil electrical conductivity and magnetic susceptibility was conducted at two depths: 0.5 and 1 m. Soil compaction was measured for a soil layer at 0–0.5 m. Relationships between electrical soil parameters and soil compaction were modelled with the use of two types of neural networks—multilayer perceptron (MLP) and radial basis function (RBF). Better prediction quality was observed for RBF models. It can be stated that in the mathematical model, the apparent soil electrical conductivity affects soil compaction significantly more than magnetic susceptibility. However, magnetic susceptibility gives additional information about soil properties, and therefore, both electrical parameters should be used simultaneously for the delimitation of management zones.



**Citation:** Pentoś, K.; Pieczarka, K.; Serwata, K. The Relationship between Soil Electrical Parameters and Compaction of Sandy Clay Loam Soil. *Agriculture* **2021**, *11*, 114. <https://doi.org/10.3390/agriculture11020114>

Academic Editor: Gniewko Niedbala

Received: 28 December 2020

Accepted: 28 January 2021

Published: 1 February 2021

**Publisher's Note:** MDPI stays neutral with regard to jurisdictional claims in published maps and institutional affiliations.



**Copyright:** © 2021 by the authors. Licensee MDPI, Basel, Switzerland. This article is an open access article distributed under the terms and conditions of the Creative Commons Attribution (CC BY) license (<https://creativecommons.org/licenses/by/4.0/>).

**Keywords:** apparent soil electrical conductivity (ECa); magnetic susceptibility (MS); EM38; neural networks

## 1. Introduction

One of the objectives of precision agriculture is optimizing production by increasing yield or by cost reduction due to optimizing the use of natural resources, and improving soil quality [1]. Another important aspect is also environmental impact reduction, e.g., by the variable-rate application of fertilizers or reduction of the application of plant protection products. For this purpose, many new technologies have been developed and used in practice. One available technique popular in precision agriculture is the delimitation of management zones. Management zones are areas of the field with similar characteristics, such as soil texture and chemical composition [2]. The optimization of crop production requires knowledge of many soil properties. These properties are very often determined by expensive and time-consuming methods. Delimitation of management zones allows for a reduction in sample numbers involved in defining soil properties. However, this process is difficult due to the high soil spatial variability and complex combination of factors that may influence soil properties [3].

Soil spatial variations may be analyzed based on many techniques such as apparent soil electrical conductivity (EC<sub>a</sub>) maps, crop yield maps and soil organic matter maps [4–6]. The electrical soil parameters are influenced by many physical-chemical features of soil. The apparent soil electrical conductivity is defined as the soil capacity for conducting electric current. EC<sub>a</sub> reflects some soil properties such as water content, bulk density, salinity, clay content, texture, organic matter content, size and distribution of pores, depth to contrasting soil layers, and organic carbon content [7–9]. Magnetic susceptibility (MS)

expresses the level of magnetization of a soil in reaction to an applied magnetic field. Magnetite and maghemite as ferromagnetic minerals are the main determinants of soil magnetic susceptibility [10]. MS is strongly affected by soil drainage class, texture, clay content, organic matter, and organic carbon [11–14].

Geospatial measurements of apparent soil electrical conductivity and magnetic susceptibility are reliable, quick, easy, nondestructive, and economic; therefore, they are recognized as a valuable mapping tool indicating soil productivity [15,16]. Furthermore, the important feature of  $EC_a$  is its temporal stability, which has been demonstrated in prior literature [17,18]. Many studies have investigated the potential of soil electrical parameters in the delimitation of management zones. Serrano et al. (2014) reported the potential usability of  $EC_a$  measurement using the Veris 2000 XA sensor for monitoring soil texture, moisture content, organic matter, pH, and phosphorus soil content [19]. Pedrera-Parrilla et al. (2016) delimited three management zones with similar soil conditions based on  $EC_a$  measurement [1]. They found an exponential relationship between spatially averaged soil water content and  $EC_a$  for water contents lower than  $0.11 \text{ kg} \cdot \text{kg}^{-1}$ . Peralta et al. (2013) reported that  $EC_a$  variability can be explained by some soil properties, namely clay content, soil organic matter, cation exchange capacity, and soil water content [15]. de Souza Bahia et al. (2017) reported a high correlation between MS and clay, iron oxides, carbon, and nitrogen, and revealed that MS is a good predictor of key properties of soils under study [20]. Magnetic susceptibility was used by some researchers for soil mapping according to the degree of contamination with heavy metals or organic compounds [21,22]. Ayoubi et al. (2019) reported a strong relationship between magnetic susceptibility and concentrations of chromium, iron, nickel, zinc, cobalt, and manganese [10]. It can be stated that the apparent electrical conductivity of soil has become one of the most popular tools for characterizing the spatial variability of soil parameters. Magnetic susceptibility is most often used for soil mapping in the context of environmental pollution.

Soil compaction may result from natural causes such as soil parameters, freezing, and drying or from mechanical operations with the use of heavy wheeled machines. As a soil compaction influences the yield, the delimitation of management zones connected with this parameter is of great importance. Soil compaction affects the water infiltration rate, soil air permeability, nitrogen availability, root length, root penetration, and rooting depth [23,24]. Soil compaction mapping is necessary, e.g., for a variable-depth tillage technology that plays an important role in applications of precision agriculture.

Artificial neural networks (ANNs) are very useful tools for solving prediction problems in agriculture, and there are many applications of neural network modelling in state-of-the-art literature. The advantage of ANNs is the ability to produce high-quality prediction models of complex and nonlinear relationships [25–27].

Generally, for the delimitation of management zones, a single electrical parameter ( $EC_a$  or MS) is used.  $EC_a$  is more popular and is connected with many physical-chemical properties of soil. However, there is still a lack of investigations regarding relationships between  $EC_a$  and MS with soil compaction. Thus, the objectives of this study are: (1) To assess whether field-scale  $EC_a$  and MS geospatial measurements are potential estimators of soil compaction and (2) to indicate the optimum set of electrical soil parameters for the delimitation of management zones connected with soil compaction.

## 2. Materials and Methods

### 2.1. Experimental Data Acquisition

The  $12.86 \text{ ha}$  ( $1.286 \times 10^5 \text{ m}^2$ ) large experimental area is located in Poland, Lower Silesia province, Olesnica district ( $51^\circ 10' 13.5'' \text{ N}$  and  $17^\circ 27' 6.6'' \text{ E}$ ). Soil sampling was carried out during the summer period of 2019. In the 2018 growing season, the area was grown with winter oilseed rape, and after combine harvesting, the field was cultivated with the universal cultivator Horsch Terrano with a depth of  $0.01 \text{ m}$ . Thereafter, until the measurement procedure, no cultivation was carried out. Soil was classified as a sandy clay

loam, according to the Polish Soil Classification System and USDA Soil Taxonomy [28]. The physical characterization of soil is shown in Table 1.

**Table 1.** Soil texture parameters.

Texture	Diameter [mm]	Percentage
skeletons	>2	1.2
sand	2–0.05	57.3
silt	0.05–0.002	18.4
clay	<0.002	24.3
soil texture	Sandy clay loam (SCL)	

The apparent soil electrical conductivity and magnetic susceptibility were measured by electromagnetic induction with the a Geonics EM38-MK2 Ground Conductivity Meter at two depths: 0.5 and 1 m. For the vertical dipole orientation used during measurements, the effective depth is 1.5 m for a coil distance of 1.0 m and 0.75 m for a coil distance of 0.5 m. The position of EM38 was registered by GPS. The technical parameters of the EM38-MK2 meter are detailed in Table 2.

**Table 2.** Technical parameters of the EM38-MK2 meter.

Measured quantities	1: Apparent conductivity in millisiemens per meter ( $\text{mS}\cdot\text{m}^{-1}$ )
	2: In-phase ratio of the secondary to primary magnetic field in parts per thousand (ppt)
Intercoil spacing	1 and 0.5 m
Operating frequency	14.5 kHz
Measuring range	Conductivity: $1000 \text{ mS}\cdot\text{m}^{-1}$ In-phase: $\pm 28$ ppt for 1 m separation In-phase: $\pm 7$ ppt for 0.5 m separation
Measurement resolution	$\pm 0.1\%$ of full scale
Measurement accuracy	$\pm 5\%$ at $30 \text{ mS}\cdot\text{m}^{-1}$
Noise levels	Conductivity: $0.5 \text{ mS}\cdot\text{m}^{-1}$ ; in-phase: 0.02 ppt

The soil compaction was measured for a soil layer 0–0.5 m with a Eijkelkamp Penetrologger with GPS. In measurements, a cone with an angle of  $60^\circ$  and a base of  $0.0001 \text{ m}^2$  was used. Penetration speed was equal to  $0.03 \text{ m}\cdot\text{s}^{-1}$ . Soil moisture was measured within a short time period after the EM38 survey and was equal to 30%.

After the measurement of electrical parameters and analysis of results, the five management zones were delimited (depicted in different colors in Figure 1). Then, the measurement of soil compaction was conducted every 30 m (measurement points are depicted in Figure 1). Based on GPS information of the penetrometer, coordinates were assigned to each measurement point. Thereafter, with the use of the least squares method, the nearest point of  $\text{EC}_a$  and MS measurement was connected to each point of the soil compaction measurement.

## 2.2. Artificial Neural Networks

An artificial neural network is a computational tool modelled on the biological functioning of the human nervous system. An ANN is made up of fundamental information-processing units called artificial neurons. Artificial neurons are arranged in layers. At least two layers are obligatory in the ANN structure—input and output layer. In this work, the two types of ANNs are used for modelling relationships under study—multilayer perceptron (MLP) and radial basis function (RBF) neural network. The MLP is a feedforward neural network with one or two hidden layers of neurons placed between the input and output layer. The MLP is trained with the use of a backpropagation algorithm. An RBF

network is a feedforward neural network with one hidden layer. Neurons in a hidden layer are RBF nonlinear activation units, usually with Gaussian functions [29]. The output signal of the RBF network is calculated by a linear neuron. RBF neural networks are considered a tool with better approximation abilities and faster learning speed than other types of ANNs [30].



**Figure 1.** The map of experimental area with management zones depicted in different colors and soil compaction measurement points.

As a result of measurements, a set of 154 data was obtained. Outliers were removed from the data set. For neural modelling, this data set was randomly divided into training and validation sets in the proportion of 80:20. Prior to the neural models training process, data were normalized into a range  $<0;1>$ . In this research, both MLP and RBF neural models were developed in the Statistica v. 13 software. The input vector was composed of a certain combination of apparent soil electrical conductivity and magnetic susceptibility measured at the depth of 0.5 and 1 m. The form of input vectors determined the number of nodes in the input layer (2 or 4). For each model, the group of 2000 neural structures was trained. Each structure was characterized by an ANN type (MLP or RBF), the number of neurons in the hidden layer (from 10 to 40), the initial connection weight matrix, and in the case of the MLP network—transfer functions of neurons in hidden and output layers (hyperbolic tangent, sigmoidal, and exponential). After the training and testing process, the neural model of the best accuracy was indicated based on the coefficient of correlation (R) between experimental data and data calculated by the neural model for the validation data set. As an output model parameter, a compaction of a certain soil layer was used.

For the indication of the optimal vector of input parameters, the determination of the contribution of independent input variables in an ANN model was necessary. For this purpose, the sensitivity analysis implemented in the Statistica v. 13 environment was employed. This method can be used for the MLP neural network to provide information about the relative importance of the input model parameters. The sensitivity analysis is based on replacing the values of each input variable by its mean values. The mean values are calculated using the training data set. Afterward, an error ratio is calculated as follows:

$$R_e = \frac{E_{ch}}{E_{oryg}} \quad (1)$$

where  $R_e$  is an error ratio,  $E_{ch}$  is a network error with a certain input changed by its mean value, and  $E_{oryg}$  is a network error with the input with its original value. Based on the error ratio  $R_e$ , the percentages of influence of the input parameters of an ANN model on its output is calculated. This method of sensitivity analysis was used, e.g., in the modelling and analysis of the structural damage after an earthquake [31].

### 3. Results and Discussion

The statistics of the experimental data (electrical and physical soil properties) are presented in Table 3.

**Table 3.** Statistics of experimental data.

The Parameter	Minimum	Maximum	Mean	Standard Deviation
apparent soil electrical conductivity 0.5 m [ $\text{mS}\cdot\text{m}^{-1}$ ]	0.39	15.23	5.10	3.05
magnetic susceptibility 0.5 m [-]	−0.11	−0.01	−0.09	0.02
apparent soil electrical conductivity 1 m [ $\text{mS}\cdot\text{m}^{-1}$ ]	0.00	36.95	8.18	6.77
magnetic susceptibility 1 m [-]	−4.18	0.16	−2.09	0.70
soil compaction (depth 0–0.1 m) [MPa]	0.17	1.03	0.40	0.17
soil compaction (depth 0–0.2 m) [MPa]	0.36	1.60	0.86	0.24
soil compaction (depth 0–0.3 m) [MPa]	0.42	2.04	1.15	0.28
soil compaction (depth 0–0.4 m) [MPa]	0.57	2.20	1.39	0.28
soil compaction (depth 0–0.5 m) [MPa]	0.65	2.20	1.41	0.28
soil compaction (depth 0.1–0.2 m) [MPa]	0.48	2.20	1.28	0.37
soil compaction (depth 0.2–0.3 m) [MPa]	0.42	3.41	1.71	0.51
soil compaction (depth 0.3–0.4 m) [MPa]	0.89	3.28	2.04	0.51
soil compaction (depth 0.4–0.5 m) [MPa]	0.17	3.39	1.14	0.58

As shown in Table 3, the apparent soil electrical conductivity is higher for the measurement depth of 1 m than for 0.5 m. The magnetic susceptibility is negative when measured at a depth of 0.5 m and changes its values from negative to positive, when measured at a depth of 1 m. Soil compaction values increase with the measurement depth when the soil layer being measured is between 0 and a certain depth. When the measurement is carried out for a soil layer of 0.1 m, the soil compaction increases with the increase in soil layer depth up to 0.4 m. The mean soil compaction of the soil layer between 0.4 and 0.5 m is similar to 0.1–0.2 m soil layer compaction. Maps of spatial variability for selected soil parameters presented in Table 3 are depicted in Figure 2.

Maps presented in Figure 2 confirm the similarity in the spatial distribution pattern for  $\text{EC}_a$  and MS, as well as for soil compaction measured at depths of 0–0.5 and 0.4–0.5 m.

An EM38-MK2 meter provides the measurement of two electrical soil parameters—apparent soil electrical conductivity and magnetic susceptibility. Generally, the apparent soil electrical conductivity is the parameter used for the delimitation of management zones. In order to establish the optimum set of parameters for the delimitation of management zones connected with soil compaction, the group of neural models was developed. As input model parameters, the following vectors were used: [ $\text{EC}_a$  0.5 m;  $\text{EC}_a$  1 m], [ $\text{EC}_a$  0.5 m; MS 0.5 m], [ $\text{EC}_a$  0.5 m; MS 0.5 m;  $\text{EC}_a$  1 m; MS 1 m], and [MS 0.5 m; MS 1 m]. As an output parameter, the soil compaction of various soil layer depths was used. The type, structure, and quality of the best neural models are summarized in Table 4.

In the process of the development of neural models, the two neural network types were used, namely the multilayer perceptron and radial basis function neural network. The data presented in Table 4 suggest that the better neural network type for modelling the relationships between soil electrical parameters and soil compaction was the RBF neural network. The number of neurons in the hidden layer varies significantly, for MLP models from 11 to 39 and for RBF models from 10 to 36.



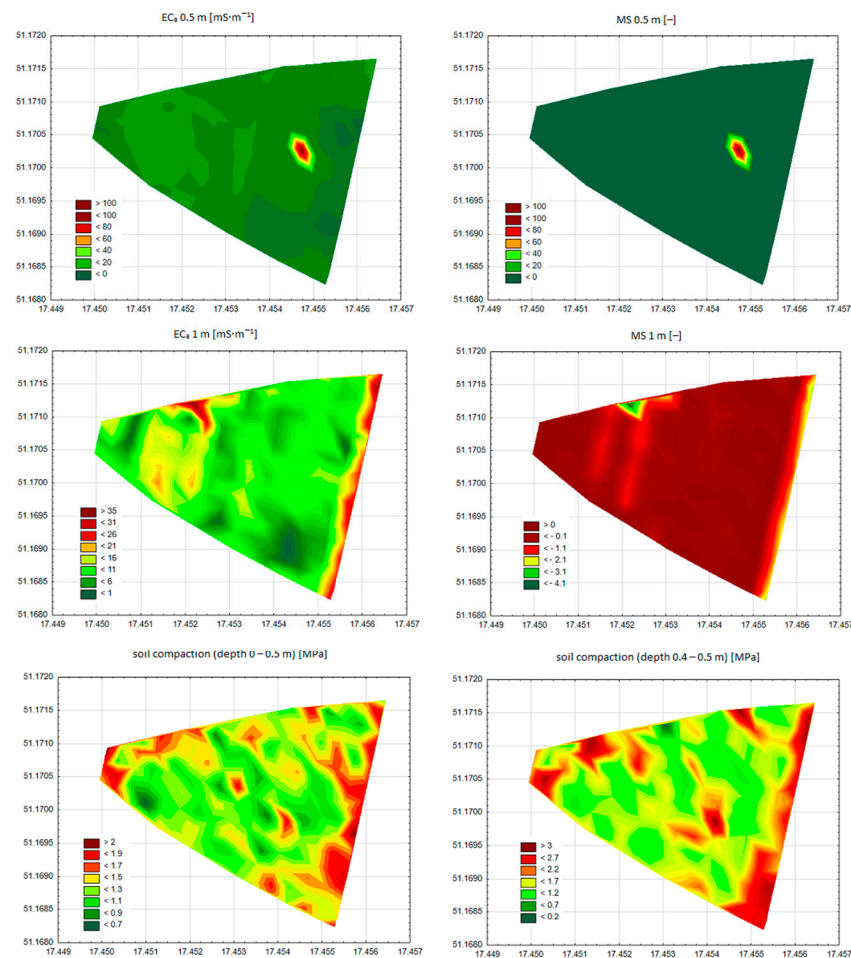


**Figure 2.** Maps of spatial variability for apparent soil electrical conductivity, magnetic susceptibility, soil compaction (0–0.5 m), and soil compaction (0.4–0.5 m).

**Table 4.** Neural models characteristics.

Input Parameters	Output Parameter	ANN Type	ANN Structure	R
EC <sub>a</sub> 0.5; MS 0.5; EC <sub>a</sub> 1; MS 1	soil compaction (0–0.5 m)	MLP	4-17-1	0.769
EC <sub>a</sub> 0.5; MS 0.5; EC <sub>a</sub> 1; MS 1	soil compaction (0.4–0.5 m)	RBF	4-14-1	0.826
EC <sub>a</sub> 0.5; MS 0.5	soil compaction (0–0.5 m)	MLP	2-20-1	0.877
EC <sub>a</sub> 0.5; MS 0.5	soil compaction (0.4–0.5 m)	MLP	2-19-1	0.846
EC <sub>a</sub> 0.5; MS 0.5	soil compaction (0–0.4 m)	RBF	2-17-1	0.700
EC <sub>a</sub> 0.5; MS 0.5	soil compaction (0–0.3 m)	RBF	2-24-1	0.446
EC <sub>a</sub> 0.5; MS 0.5	soil compaction (0–0.2 m)	RBF	2-10-1	0.521
EC <sub>a</sub> 0.5; MS 0.5	soil compaction (0–0.1 m)	RBF	2-20-1	0.615
EC <sub>a</sub> 0.5; MS 0.5	soil compaction (0.3–0.4 m)	RBF	2-33-1	0.662
EC <sub>a</sub> 0.5; MS 0.5	soil compaction (0.2–0.3 m)	MLP	2-12-1	0.594
EC <sub>a</sub> 0.5; MS 0.5	soil compaction (0.1–0.2 m)	RBF	2-36-1	0.476
EC <sub>a</sub> 0.5; EC 1	soil compaction (0–0.5 m)	RBF	2-27-1	0.759
EC <sub>a</sub> 0.5; EC 1	soil compaction (0.4–0.5 m)	RBF	2-11-1	0.732
EC <sub>a</sub> 0.5; EC 1	soil compaction (0–0.4 m)	RBF	2-28-1	0.656
EC <sub>a</sub> 0.5; EC 1	soil compaction (0–0.3 m)	RBF	2-21-1	0.517
EC <sub>a</sub> 0.5; EC 1	soil compaction (0–0.2 m)	RBF	2-15-1	0.433
EC <sub>a</sub> 0.5; EC 1	soil compaction (0–0.1 m)	MLP	2-16-1	0.501
EC <sub>a</sub> 0.5; EC 1	soil compaction (0.3–0.4 m)	RBF	2-21-1	0.648
EC <sub>a</sub> 0.5; EC 1	soil compaction (0.2–0.3 m)	RBF	2-27-1	0.470
EC <sub>a</sub> 0.5; EC 1	soil compaction (0.1–0.2 m)	RBF	2-12-1	0.471
MS 0.5; MS 1	soil compaction (0–0.5 m)	RBF	2-10-1	0.725
MS 0.5; MS 1	soil compaction (0.4–0.5 m)	MLP	2-39-1	0.790

The input parameters: Apparent soil electrical conductivity, 0.5 m; magnetic susceptibility, 0.5 m; apparent soil electrical conductivity, 1 m; and magnetic susceptibility, 1 m are marked in the table as EC<sub>a</sub> 0.5, MS 0.5, EC<sub>a</sub> 1, and MS 1, respectively.

Taking into account the fact that electrical parameters were measured at depths of 0.5 and 1 m, it can be expected that a better quality of models is obtained when the output model parameter is the soil compaction measured at a depths of 0–0.5 and 0.4–0.5 m. It was confirmed by the results summarized in Table 4. For an apparent soil electrical conductivity of 0.5 m and magnetic susceptibility of 0.5 m, as well as for apparent soil electrical conductivities of 0.5 and 1 m as input model parameters, the nine neural models were developed with soil compaction measured for each soil layer described in the section ‘Materials and Methods’. The model quality increases when soil compaction is measured at greater depths. Only when the output model parameter is the soil compaction measured for a soil layer of 0–0.5 and 0.4–0.5 m is the correlation coefficient  $R$  for the validation data set greater than 0.7. The high  $R$  value calculated for the validation data set proves the model usefulness for real-life applications and means that no overfitting effect occurred during the training process. Based on the results described above, for magnetic susceptibility, 0.5 and 1 m, as well as for a combination of all electrical parameters as input vector components, only soil compaction measured for soil layers of 0–0.5 and 0.4–0.5 m was taken into account as an output parameter of neural models. In the case of magnetic susceptibility, 0.5 and 1 m as input model parameters, the values of correlation between predicted and experimental soil compaction equal 0.725 for the soil layer at 0–0.5 m and 0.790 for the soil layer at 0.4–0.5 m. When all electrical parameters were input vector components, the  $R$  values were 0.769 for the soil layer at 0–0.5 m and 0.826 for the soil layer at 0.4–0.5 m. The highest quality of models was obtained for an apparent soil electrical conductivity at 0.5 m and magnetic susceptibility at 0.5 m as input model parameters. This means that both electrical parameters play important roles in the delimitation of management zones. A slightly lower quality of models was calculated in the case of these two electrical parameters measured at depths of 0.5 and 1 m. It can be assumed that the quality of these models could increase for soil compaction measured at a depth between 0.5 and 1 m. However, soil compaction measured in deeper soil layers is of no practical relevance, because of limitations in rooting depth, as well as characteristics of the working resistance of soil-working machines.

Based on the model of the relationship between apparent soil electrical conductivity and magnetic susceptibility measured at depths of 0.5 and 1 m, and soil compaction 0–0.5 m, the sensitivity analysis was performed in order to determine the average variable relative importance. The results are depicted in Figure 3.

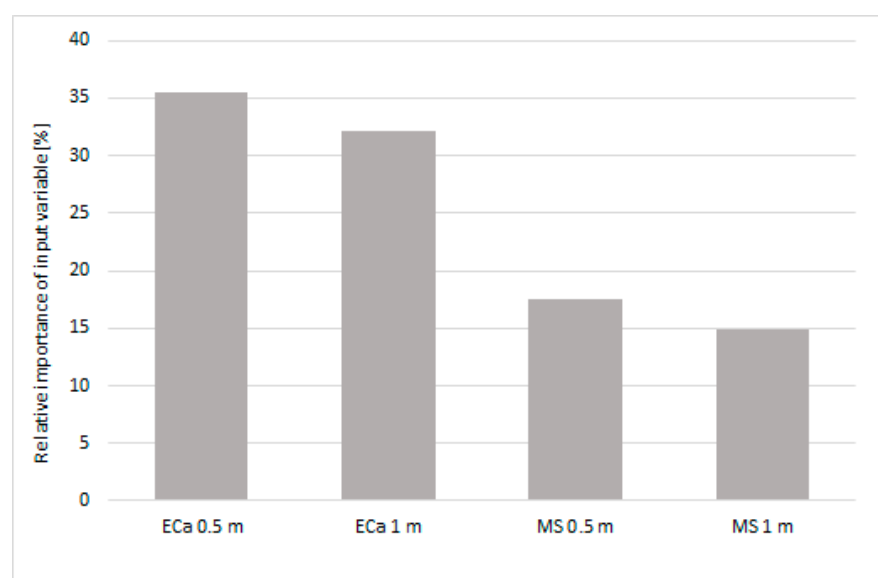


**Figure 3.** The relative importance of input variables of multilayer perceptron (MLP) model on soil compaction (0–0.5 m).

As illustrated in Figure 3, apparent soil electrical conductivity affects soil compaction about twice as much as magnetic susceptibility. Electrical parameters measured at a depth of 0.5 m influence the compaction of the soil layer at 0–0.5 m slightly more than electrical parameters measured at a depth of 1 m. Soil compaction is affected by many physical, chemical and biological properties of soils, namely water content, organic matter content, mineralogy, soil structure and texture, and particle-size distribution [32]. These parameters also influence soil electrical parameters. Therefore, a close relation between soil compaction and both soil apparent electrical conductivity and magnetic susceptibility can be expected. The correlation between the compaction and electrical resistivity of noncohesive soils was investigated by Kowalczyk et al. (2014) [33]. Al-Gaadi et al. (2012) proved the possibility of assessing soil compaction by  $EC_a$  measured by a EM38-MK2 device [34]. The level of correlation between  $EC_a$  and soil compaction depends on the EM38-MK2 orientation (vertical or horizontal), moisture content, and the height of the device above the ground. Keskin et al. (2011) found a negative correlation between tillage depth, which depends on soil compaction and soil electrical conductivity [35]. The correlation coefficient ranged from  $R = -0.56$  to  $R = -0.84$  depending, inter alia, on the depth of electrical conductivity measurement. The authors stated that the electrical conductivity measurement system can be used for tillage depth determination.

Electrical soil parameters are increasingly popular for the delimitation of management zones in precision agriculture. Some measuring instruments were developed for this purpose. Some of them measure only one parameter (apparent soil electrical conductivity or magnetic susceptibility). Some instruments allow the measurement of both those parameters (e.g., Geonics EM38). Therefore, various surveys have been presented in the literature for the delimitation of management zones. Guo et al. (2019) presented a geostatistical method combined with a fuzzy clustering algorithm for determination of the spatiotemporal variation of soil salinity based on  $EC_a$  measurement conducted with the EM38 tool [36]. Machado et al. (2015) reported a relatively high linear correlation ( $R = 0.778$ ) between  $EC_a$  measured by the EMP-400 profiler sensor at 15 kHz and cation exchange capacity. They found a lower correlation between  $EC_a$  and other soil parameters, namely organic matter, potassium, and base saturation [37]. Valente et al. (2014) indicated  $EC_a$  as an important tool for defining management zones due to its significant correlation with the micronutrients manganese, zinc and copper, as well as with macronutrients potassium and phosphorus [6]. They also found a strong correlation of  $EC_a$  with the remaining phosphorus. It proves the usability of  $EC_a$  measurement in precision fertilizer application. Grimley et al. (2004) used only magnetic susceptibility for the delineation of hydric soils in the midwestern USA. They found the critical MS values for differentiation of silty and sandy surface soil textures [11]. Soderstrom et al. (2013) used  $EC_a$ , MS, and gamma ray data for mapping soil properties. They reported that  $EC_a$  and MS were better indicators of soil properties under study than gamma ray measurements [38]. Jordanova et al. (2013) suggested that the combination of  $EC_a$  and magnetic soil parameters can improve the process of soil classification by decreasing the nonunique interpretation of the relationship between apparent conductivity and certain soil physical properties [39].

Artificial neural networks have been employed by many researchers for prediction of soil properties and, based on results, ANNs have been introduced as an efficient model of relationships under study. In our research, the correlation coefficient  $R$  does not exceed 0.877, which is not a very high correlation when compared with other neural prediction models evaluated by authors [40,41]. It can be assumed that in addition to the soil parameters reflected by  $EC_a$  and MS, other soil features influence the soil compaction. Similar or lower neural models' quality was reported in a prior literature for ANNs as a tool for the prediction of soil properties. Khanbabakhani et al. (2020) indicated ANNs as an efficient model of the relationship between soil texture and longitude, altitude, elevation, and slope percentage. They compared an ANN model with three other interpolation methods including inverse distance weighting, kriging, and co-kriging used for soil texture mapping. Based on statistical indices, the efficiency of the ANN model was better than



other methods. However, the correlation of the model was less than 0.5 [42]. A feed-forward back-propagation network with one hidden layer was used by Aitkenhead et al. (2015) as a predictive model of soil organic matter [43]. They calculated different qualities of models depending on values of organic matter in the training data set. For a full-organic-matter-content-range model, they reported  $R = 0.93$ , and for a small-organic-matter-content model (less than 20%),  $R = 0.82$ . Tasan et al. (2020) used a MLP neural network for the prediction of soil moisture described by two parameters, namely field capacity and permanent wilting point [44]. Among the ANN models developed in this research, a model with four input parameters (sand, clay, percent calcium carbonate, and cation exchange capacity) yielded the greatest quality ( $R = 0.88$  for field capacity and  $R = 0.81$  for permanent wilting point as output parameter of model).

#### 4. Conclusions

In recent literature, there is a lack of scientific papers regarding relationships between electrical parameters and soil compaction. Therefore, in this research, two parameters:  $EC_a$  and MS, as potential estimators of soil compaction were investigated. The spatial variability maps present similar patterns for apparent soil electrical conductivity and magnetic susceptibility, both measured at a depth of 0.5 m. A similar pattern was also found for soil compaction measured at a depth of 0–0.5 m, and soil compaction measured at a depth of 0.4–0.5 m. The neural models of high quality were developed for prediction of soil compaction measured for soil layers at 0–0.5 and 0.4–0.5 m based on electrical parameters of the soil. The RFB neural network turned out to be a better prediction tool for this purpose. In the mathematical model, the apparent soil electrical conductivity affects soil compaction significantly more than magnetic susceptibility. In spite of this fact, MS provides additional information about soil properties. Therefore, MS should be used as a complementary parameter to  $EC_a$  in the process of the delimitation of management zones. It can be concluded that the measurement of  $EC_a$  and MS can be considered a relatively inexpensive, easy, and fast technique with the potential to make significant contributions to the identification and prediction of soil compaction. This technique is promising for real-life applications, e.g., for variable-depth tillage technology based on soil compaction mapping that can reduce fuel consumption.

**Author Contributions:** Conceptualization, K.P. (Katarzyna Pentoś), K.P. (Krzysztof Pieczarka) and K.S.; data curation, K.P. (Katarzyna Pentoś), K.P. (Krzysztof Pieczarka) and K.S.; formal analysis, K.P. (Katarzyna Pentoś) and K.P. (Krzysztof Pieczarka); investigation, K.P. (Katarzyna Pentoś), K.P. (Krzysztof Pieczarka) and K.S.; methodology, K.P. (Katarzyna Pentoś), K.P. (Krzysztof Pieczarka) and K.S.; writing—original draft, K.P. (Katarzyna Pentoś); writing—review and editing, K.P. (Katarzyna Pentoś) and K.P. (Krzysztof Pieczarka); visualization, K.P. (Katarzyna Pentoś) and K.P. (Krzysztof Pieczarka). All authors have read and agreed to the published version of the manuscript.

**Funding:** This research received no external funding.

**Institutional Review Board Statement:** Not applicable.

**Informed Consent Statement:** Not applicable.

**Data Availability Statement:** Data are available by contacting the authors.

**Conflicts of Interest:** The authors declare no conflict of interest.

#### References

1. Pedrera-Parrilla, A.; Brevik, E.C.; Giraldez, J.V.; Vanderlinden, K. Temporal stability of electrical conductivity in a sandy soil. *Int. Agrophys.* **2016**, *30*, 349–357. [\[CrossRef\]](#)
2. Moral, F.J.; Terron, J.M.; da Silva, J.R.M. Delineation of management zones using mobile measurements of soil apparent electrical conductivity and multivariate geostatistical techniques. *Soil. Till. Res.* **2010**, *106*, 335–343. [\[CrossRef\]](#)
3. Brevik, E.C.; Calzolari, C.; Miller, B.A.; Pereira, P.; Kabala, C.; Baumgarten, A.; Jordan, A. Soil mapping, classification, and pedologic modeling: History and future directions. *Geoderma* **2016**, *264*, 256–274. [\[CrossRef\]](#)
4. Dalchiavon, F.C.; Carvalho, M.D.E.; Montanari, R.; Andreotti, M. Strategy of specification of management areas: Rice grain yield as related to soil fertility. *Rev. Bras. Cienc. Solo* **2013**, *37*, 45–54. [\[CrossRef\]](#)

5. Fleming, K.L.; Heermann, D.F.; Westfall, D.G. Evaluating soil color with farmer input and apparent soil electrical conductivity for management zone delineation. *Agron. J.* **2004**, *96*, 1581–1587. [\[CrossRef\]](#)
6. Valente, D.S.M.; De Queiroz, D.M.; Pinto, F.D.D.; Santos, F.L.; Santos, N.T. Spatial variability of apparent electrical conductivity and soil properties in a coffee production field. *Eng. Agric.* **2014**, *34*, 1224–1233. [\[CrossRef\]](#)
7. Bertermann, D.; Schwarz, H. Laboratory device to analyse the impact of soil properties on electrical and thermal conductivity. *Int. Agrophys.* **2017**, *31*, 157–166. [\[CrossRef\]](#)
8. Kuhn, J.; Brenning, A.; Wehrhan, M.; Koszinski, S.; Sommer, M. Interpretation of electrical conductivity patterns by soil properties and geological maps for precision agriculture. *Precis. Agric.* **2009**, *10*, 490–507. [\[CrossRef\]](#)
9. Martinez, G.; Vanderlinden, K.; Ordonez, R.; Muriel, J.L. Can Apparent Electrical Conductivity Improve the Spatial Characterization of Soil Organic Carbon? *Vadose Zone J.* **2009**, *8*, 586–593. [\[CrossRef\]](#)
10. Ayoubi, S.; Adman, V.; Yousefifard, M. Use of magnetic susceptibility to assess metals concentration in soils developed on a range of parent materials. *Ecotox. Environ. Safe.* **2019**, *168*, 138–145. [\[CrossRef\]](#)
11. Grimley, D.A.; Arruda, N.K.; Bramstedt, M.W. Using magnetic susceptibility to facilitate more rapid, reproducible and precise delineation of hydric soils in the midwestern USA. *Catena* **2004**, *58*, 183–213. [\[CrossRef\]](#)
12. Siqueira, D.S.; Marques, J.; Matias, S.S.R.; Barron, V.; Torrent, J.; Baffa, O.; Oliveira, L.C. Correlation of properties of Brazilian Haplustalfs with magnetic susceptibility measurements. *Soil Use Manag.* **2010**, *26*, 425–431. [\[CrossRef\]](#)
13. Maher, B.A. Magnetic properties of modern soils and Quaternary loessic paleosols: Paleoclimatic implications. *Palaeogeogr. Palaeoclimatol.* **1998**, *137*, 25–54. [\[CrossRef\]](#)
14. Yang, P.G.; Yang, M.; Mao, R.Z.; Byrne, J.M. Impact of Long-Term Irrigation with Treated Sewage on Soil Magnetic Susceptibility and Organic Matter Content in North China. *Bull. Environ. Contam. Tox.* **2015**, *95*, 102–107. [\[CrossRef\]](#)
15. Peralta, N.R.; Costa, J.L.; Balzarini, M.; Angelini, H. Delineation of management zones with measurements of soil apparent electrical conductivity in the southeastern pampas. *Can. J. Soil. Sci.* **2013**, *93*, 205–218. [\[CrossRef\]](#)
16. Molin, J.P.; de Castro, C.N. Establishing management zones using soil electrical conductivity and other soil properties by the fuzzy clustering technique. *Sci. Agric.* **2008**, *65*, 567–573. [\[CrossRef\]](#)
17. De Caires, S.A.; Wuddivira, M.N.; Bekele, I. Spatial analysis for management zone delineation in a humid tropic cocoa plantation. *Precis. Agric.* **2015**, *16*, 129–147. [\[CrossRef\]](#)
18. Li, Y.; Shi, Z.; Li, F. Delineation of site-specific management zones based on temporal and spatial variability of soil electrical conductivity. *Pedosphere* **2007**, *17*, 156–164. [\[CrossRef\]](#)
19. Serrano, J.; Shahidian, S.; da Silva, J.M. Spatial and Temporal Patterns of Apparent Electrical Conductivity: DUALEM vs. Veris Sensors for Monitoring Soil Properties. *Sensors* **2014**, *14*, 10024–10041. [\[CrossRef\]](#)
20. De Souza Bahia, A.S.R.; Marques, J.; La Scala, N.; Cerri, C.E.P.; Camargo, L.A. Prediction and Mapping of Soil Attributes using Diffuse Reflectance Spectroscopy and Magnetic Susceptibility. *Soil Sci. Soc. Am. J.* **2017**, *81*, 1450–1462. [\[CrossRef\]](#)
21. Wang, X.S. Magnetic properties and heavy metal pollution of soils in the vicinity of a cement plant, Xuzhou (China). *J. Appl. Geophys.* **2013**, *98*, 73–78. [\[CrossRef\]](#)
22. Sarris, A.; Kokinou, E.; Aidona, E.; Kallithrakas-Kontos, N.; Koulouridakis, P.; Kakoulaki, G.; Droulia, K.; Damianovits, O. Environmental study for pollution in the area of Megalopolis power plant (Peloponnesos, Greece). *Environ. Geol.* **2009**, *58*, 1769–1783. [\[CrossRef\]](#)
23. Tan, X.; Chang, S.X.; Kabzems, R. Soil compaction and forest floor removal reduced microbial biomass and enzyme activities in a boreal aspen forest soil. *Biol. Fert. Soils* **2008**, *44*, 471–479. [\[CrossRef\]](#)
24. Kristoffersen, A.O.; Riley, H. Effects of soil compaction and moisture regime on the root and shoot growth and phosphorus uptake of barley plants growing on soils with varying phosphorus status. *Nutr. Cycl. Agroecosys.* **2005**, *72*, 135–146. [\[CrossRef\]](#)
25. Niedbala, G.; Nowakowski, K.; Rudowicz-Nawrocka, J.; Piekutowska, M.; Weres, J.; Tomczak, R.J.; Tyksiński, T.; Álvarez, P.A. Multicriteria Prediction and Simulation of Winter Wheat Yield Using Extended Qualitative and Quantitative Data Based on Artificial Neural Networks. *Appl. Sci.* **2019**, *9*, 2773. [\[CrossRef\]](#)
26. Niedbala, G.; Piekutowska, M.; Weres, J.; Korzeniewicz, R.; Witaszek, K.; Adamski, M.; Pilarski, K.; Czechowska-Kosacka, A.; Krysztofiak-Kaniewska, A. Application of Artificial Neural Networks for Yield Modeling of Winter Rapeseed Based on Combined Quantitative and Qualitative Data. *Agronomy* **2019**, *9*, 781. [\[CrossRef\]](#)
27. Wang, L.; Wang, P.X.; Liang, S.L.; Zhu, Y.C.; Khan, J.; Fang, S.B. Monitoring maize growth on the North China Plain using a hybrid genetic algorithm-based back-propagation neural network model. *Comput. Electron. Agric.* **2020**, *170*. [\[CrossRef\]](#)
28. Distribution, P.S. Particle size distribution and textural classes of soils and mineral materials-classification of Polish Society of Soil Science (2009) *Annals of. Soil Sci.* **2009**, *60*, 5–16.
29. Faris, H.; Aljarah, I.; Mirjalili, S. Evolving radial basis function networks using moth-flame optimizer. In *Handbook of Neural Computation*; Academic Press: Cambridge, MA, USA, 2017; pp. 537–550. [\[CrossRef\]](#)
30. Ahmadian, A.S. Numerical Modeling and Simulation. In *Numerical Models for Submerged Breakwaters*; Ahmadian, A.S., Ed.; Butterworth-Heinemann: Oxford, UK, 2016; pp. 109–126.
31. Hadzima-Nyarko, M.; Nyarko, E.K.; Moric, D. A neural network based modelling and sensitivity analysis of damage ratio coefficient. *Expert Syst. Appl.* **2011**, *38*, 13405–13413. [\[CrossRef\]](#)
32. Nawaz, M.F.; Bourrie, G.; Trolard, F. Soil compaction impact and modelling. A review. *Agron. Sustain. Dev.* **2013**, *33*, 291–309. [\[CrossRef\]](#)

33. Kowalczyk, S.; Maslakowski, M.; Tucholka, P. Determination of the correlation between the electrical resistivity of non-cohesive soils and the degree of compaction. *J. Appl. Geophys.* **2014**, *110*, 43–50. [[CrossRef](#)]
34. Al-Gaadi, K. Employing Electromagnetic Induction Technique for the Assessment of Soil Compaction. *Americ. J. Agric. Biol. Sci.* **2012**, *7*, 425–434.
35. Keskin, S.; Khalilian, A.; Han, Y.J.; Dodd, R. Variable-depth Tillage based on Geo-referenced Soil Compaction Data in Coastal Plain Soils. *Int. J. Appl. Sci. Tech.* **2011**, *1*, 22–32.
36. Guo, Y.; Zhou, Y.; Zhou, L.Q.; Liu, T.; Wang, L.G.; Cheng, Y.Z.; He, J.; Zheng, G.Q. Using proximal sensor data for soil salinity management and mapping. *J. Integr. Agric.* **2019**, *18*, 340–349. [[CrossRef](#)]
37. Machado, F.C.; Montanari, R.; Shiratsuchi, L.S.; Lovera, L.H.; Lima, E.D. Spatial dependence of electrical conductivity and chemical properties of the soil by electromagnetic induction. *Rev. Bras. Cienc. Solo* **2015**, *39*, 1112–1120. [[CrossRef](#)]
38. Soderstrom, M.; Eriksson, J.; Isendahl, C.; Araujo, S.R.; Rebellato, L.; Schaan, D.P.; Stenborg, P. Using proximal soil sensors and fuzzy classification for mapping Amazonian Dark Earths. *Agric. Food Sci.* **2013**, *22*, 380–389. [[CrossRef](#)]
39. Jordanova, D.; Jordanova, N.; Werban, U. Environmental significance of magnetic properties of Gley soils near Rosslau (Germany). *Environ. Earth Sci.* **2013**, *69*, 1719–1732. [[CrossRef](#)]
40. Pentos, K.; Pieczarka, K.; Lejman, K. Application of Soft Computing Techniques for the Analysis of Tractive Properties of a Low-Power Agricultural Tractor under Various Soil Conditions. *Complexity* **2020**, *2020*. [[CrossRef](#)]
41. Cieniawska, B.; Pentos, K.; Luczycka, D. Neural modeling and optimization of the coverage of the sprayed surface. *Bull. Pol. Acad. Sci. Tech.* **2020**, *68*, 601–608. [[CrossRef](#)]
42. Khanbabakhani, E.; Torkashvand, A.M.; Mahmoodi, M.A. The possibility of preparing soil texture class map by artificial neural networks, inverse distance weighting, and geostatistical methods in Gavoshan dam basin, Kurdistan Province, Iran. *Arab. J. Geosci.* **2020**, *13*. [[CrossRef](#)]
43. Aitkenhead, M.J.; Donnelly, D.; Sutherland, L.; Miller, D.G.; Coull, M.C.; Black, H.I.J. Predicting Scottish topsoil organic matter content from colour and environmental factors. *Eur. J. Soil Sci.* **2015**, *66*, 112–120. [[CrossRef](#)]
44. Tasan, S.; Demir, Y. Comparative Analysis of MLR, ANN, and ANFIS Models for Prediction of Field Capacity and Permanent Wilting Point for Bafra Plain Soils. *Commun. Soil Sci. Plan.* **2020**, *51*, 604–621. [[CrossRef](#)]